Title: Multi-Hazard System Reliability of Flood Control Levees

Author names and affiliations: Paolo Zimmaro[a], Jonathan P. Stewart[a], Scott J. Brandenberg[a], Dong Youp Kwak[b], Ruben Jongejan[c]

[a]Department of Civil and Environmental Engineering, University of California Los Angeles, 5731 Boelter Hall, Los Angeles, CA 90095-1593, USA, *pzimmaro@ucla.edu*; *jstewart@seas.ucla.edu; sjbrandenberg@ucla.edu*

[b]Department of Civil and Environmental Engineering, Hanyang University, Ansan, Gyeonggi-do, 15588, South Korea, *dkwak@hanyang.ac.kr*

[c]Jongejan Risk Management Consulting, Schoolstraat 4, 2611 HS Delft, The Netherlands, *ruben.jongejan@jongejanrmc.com*

Corresponding author: Paolo Zimmaro, Department of Civil and Environmental Engineering, University of California Los Angeles, 5731 Boelter Hall, Los Angeles, CA 90095-1593, USA *pzimmaro@ucla.edu*

Keywords: System reliability; Level-crossing statistics; Monte Carlo simulations; Flood-Control levees; Distributed infrastructure.

Accepted for publication – Soil Dynamics and Earthquake Engineering

Multi-Hazard System Reliability of Flood Control Levees

Paolo Zimmaro[a], Jonathan P. Stewart[a], Scott J. Brandenberg[a], Dong Youp Kwak[b], Ruben Jongejan[c]

[a]Department of Civil and Environmental Engineering, University of California Los Angeles, 5731 Boelter Hall, Los Angeles, CA 90095-1593, USA

[b]Department of Civil and Environmental Engineering, Hanyang University, Ansan, Gyeonggi-do, 15588, South Korea

[c]Jongejan Risk Management Consulting, Schoolstraat 4, 2611 HS Delft, The Netherlands

Abstract: In risk assessment of spatially distributed infrastructure, the probability of demand exceeding capacity is evaluated across the system. We describe and compare two levee system reliability analysis frameworks for seismic and high-water demands. The first approach considers spatial correlations and distributions of demand and capacity between "segments" (i.e., elemental levee lengths) through Monte Carlo simulation. We apply a capacity correlation model derived from seismic case histories in Japan. The seismic demand correlation model is based on global ground motion data, whereas the high-water correlation is taken as unity. The second approach examines the distribution and correlation of capacities and demands between physics-based "reaches" (i.e., length of levee having uniform statistical distributions of capacity and demand). Statistics and spatial correlation of the limit state function are computed using a first-order reliability method procedure. The probability of failure of the reach is then computed using level-crossing statistics. For implementation of level-crossing statistics, we replace Markov-type correlation functions for levee capacity with a Gaussian function. We illustrate both methods for a levee system subjected to realistic demand and capacity distributions and show that characteristic lengths (defined as lengths of levee that can be considered as statistically independent) are comparable for high-water and seismic demands. This outcome is specific to the considered failure mechanisms and is driven by use of similar capacity correlation models, whereas differences in demand correlation models have limited impact.

1. Introduction

Levees are defined as man-made or natural embankments along rivers or water bodies. Their primary purpose is to provide protection against flood events. The performance of levees when subjected to flood or earthquakes is essential for the resilience of surrounding communities.

Despite their critical function, many levees were not engineered at the time of their construction and are often founded on soft and weak soils. As a result, levees are frequently damaged during high-water events (e.g., [1-3]) and following major earthquakes (e.g., [4-8]).

For levees that continuously impound water, a single failure anywhere along their length will produce flooding, and hence comprises system failure. For levees that intermittently impound water, the seismic failure probability is related to the combination of seismic deformation potential and probability of high water during or shortly following the event, whereas the high-water failure probability is simply the single-segment failure probability during a high-water event. In either case (continuously or intermittently loaded), levees constitute a spatially distributed series system, which present particular challenges for reliability assessment. This paper describes two conceptually similar approaches for analysis of levee reliability, with an emphasis on the system probability of failure given knowledge of capacity and demand on a more local level. We defer to other documents for recommended analysis procedures for computing capacity at the segment, or cross-section level (Zimmaro et al. [9] for seismic, URS Corporation, Jack R. Benjamin & Associates Inc. [10] for high-water).

Demands imposed on levee systems (e.g. high water related to flood events, earthquake shaking) are spatially correlated in a manner that reflects attributes of the event initiating the demand. Moreover, the available capacities of a portion of the levee to resist demands (e.g., erodibility, liquefaction susceptibility, etc.) are also spatially correlated due to the geologic depositional processes and the manner in which levee fills were constructed.

Several approaches can be used to consider spatial correlation of demand and capacity in levee systems. We take spatial demand correlation for high water events as unity [11]. For seismic demands, models for spatial correlation of ground motions are applied [12]. The correlation of capacity may be calculated based on spatial correlation of the soil properties that give rise to the levee capacity (e.g., [11, 13]), or by back-calculation of the capacity distribution based on observed damage and demand distributions [14]. We adopt the latter approach for the present work.

We present here a levee system reliability analysis framework applied at two levels of resolution. The first (Monte Carlo simulation) is computationally demanding, but more flexible. This approach generates random realizations of demand and capacity of levee segments

compatible with spatial correlation models, and then numerically calculates the probability of failure. The second is less computationally demanding, but rests on a linear approximation of the limit state function. This approach is based on the First Order Reliability Method (FORM) and level-crossing statistics.

We present both approaches using consistent terminology, which is provided next. We describe the development of capacity distributions and correlation functions, which are required elements of both the Monte Carlo and FORM methods. For a hypothetical levee system subject to specified scenario demands, we then compare results of reliability analysis for seismic and high-water events using the two methods. This paper builds upon a previous paper [15] that used a less developed version of the capacity correlation model, different levee configurations, and which considered only earthquake demands. This paper is similar to a paper in the conference proceedings [16], although the example problem has been updated.

2. Levee System Taxonomy

We apply the following terms for use in the engineering evaluation of levee reliability [15]:

- System: A length of levee that protects a particular region from flooding. A breach anywhere within the system constitutes system failure if the levee impounds water.
- Reach (Physics-Based): A length of levee that exhibits uniformity in the statistical distributions of levee capacity (soil properties, geometry), and demand (flood level, earthquake shaking, etc.). Capacity and demand vary randomly within a reach, but their statistical distributions are uniform. A two-dimensional cross-section analysis must be interpreted in a manner that considers the out-of-plane variation in capacity and demand to draw meaningful conclusions about the probability of failure of a reach.
- Reach (Legal/Jurisdictional): Levee systems are sometimes divided into "reaches" based on specific legal or jurisdictional boundaries, or other considerations that are unrelated to the physics that drive reliability analysis. It is important to distinguish this definition from the physics-based definition, and to use the physics-based definition in reliability analysis.
- Characteristic length: A characteristic length is a specific length of levee for which the probability of system failure computed based on the assumption of statistical independence of each characteristic length is equal to the probability of system failure based on a more

robust reliability analysis that considers spatial correlation of capacity and demand within the system. The probability of system failure using the characteristic length method is computed based on a simple product sum. However, the characteristic length can strictly only be defined by first computing the probability of system failure using a robust reliability analysis framework, and subsequently calculating the characteristic length. The characteristic length depends on the spatial variations of capacity and demand within the system, and is generally different for different loading conditions. In practice, a specific characteristic length has been assumed from the outset to facilitate relatively simple analyses. Errors in the selection of characteristic length directly affect the computed probability of system failure.

- Segment: A segment is a length of levee with uniform capacity and demand, and can be considered as an elemental length. A segment may be represented as a two-dimensional cross-section in engineering analysis. Soil properties may vary within a segment due to stratigraphy and depositional variability, but the capacity of the segment is constant because the size of the failure mass is large enough to average out the spatial variations in soil properties. Segments are shorter than reaches, and reaches may be analyzed as a collection of segments. The capacity among various segments is spatially correlated due to similarities in the depositional environment of the foundation soils and levee construction practices.

Note that different definitions may be found in literature for similar concepts (e.g., ‘reach’ as ‘section’, [13]).

Figure 1 shows a schematic of a levee system that is divided into multiple reaches. Each reach can be subdivided into segments, and a characteristic length may be computed from reliability analysis. In this case, we assume that a reach > characteristic length > segment, though reaches are not necessarily longer than characteristic lengths by definition.

3. Levee System Reliability Assessment Procedures

System reliability analysis consists of calculating the probability that one or more segments within the system experience failure due to a stressing event. In this paper, we focus on failure probabilities conditioned on the stressing event (denoted E), not the failure probability itself.

Important aspects of this calculation are the distribution functions of capacity and demand for the segments, and spatial correlation of capacity and demand among segments. To illustrate the importance of spatial correlation on system reliability analysis, consider two extreme cases: the capacity and demand distributions of two different segments are either perfectly correlated or statistically independent. For the case of perfect correlation, the capacity of each segment is a uniform number of standard deviations above or below the mean value, as is the demand. Hence, the conditional probability of system failure [i.e, P(F_{sys}|E)] is equal to the maximum of the conditional probabilities of failure of the individual segments in the system. In the case of statistical independence, P(F_{sys}|E) is equal to the complement of system survival, which in turn is the product of each individual segment surviving. The conditional probability of failure associated with these scenarios lies between the two extremes, which are known as uni-modal bounds for a series system [17]:

$$\max\left[\mathrm{P}\left(F_{Seg,i}|\mathrm{E}\right)\right]_{i=1:n} \le \mathrm{P}\left(F_{sys}|\mathrm{E}\right) \le 1 - \prod_{i=1}^{n}\left(1 - \mathrm{P}\left(F_{Seg,i}|\mathrm{E}\right)\right) \quad (1)$$

where arguments F_{sys} and $F_{Seg,i}$ indicate failure of the system and segment i, respectively, and n is the total number of segments. When segment capacity and/or demand are spatially correlated, the system failure probability lies between these bounds.

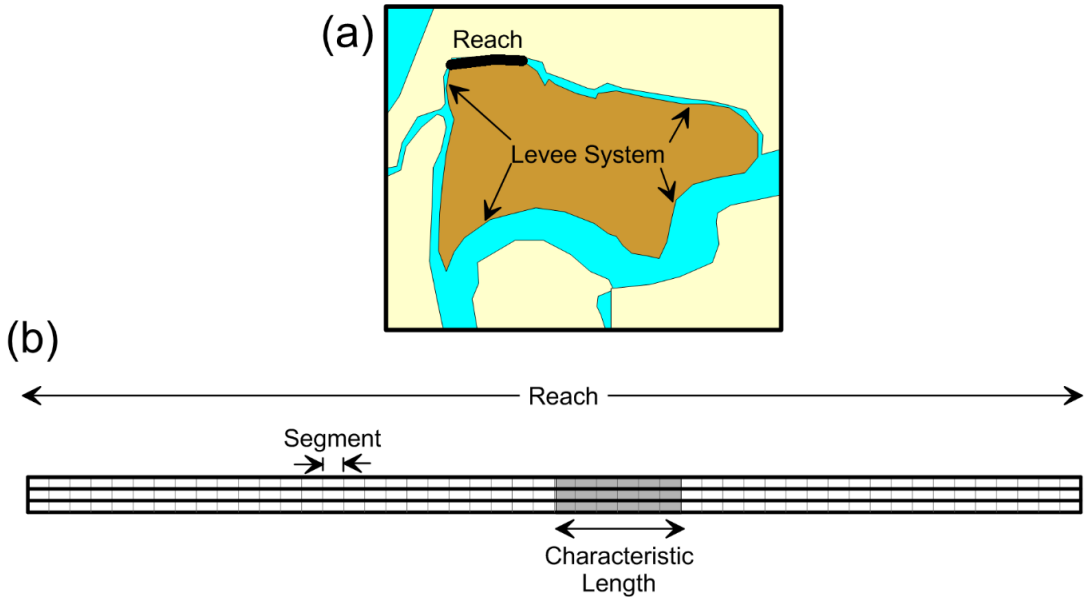

Figure 1. Definition of (a) levee system and reach; (b) levee segment and characteristic length within a reach. Adapted from Kwak et al. [15].

The range of failure probabilities provided by Eq. (1) is often wide. For example, a system composed of 10 segments each with P(F_{Seg}|E) = 0.05 will have P(F_{sys}|E) = 0.05 for perfect correlation and P(F_{sys}|E) = 0.40 for statistical independence. In general, P(F_{Seg}|E) will vary within the system, but is selected to be constant for this simple illustration. Where the actual value of P(F_{sys}|E) falls between these uni-modal bounds depends strongly on capacity and demand correlations among segments. The following sections describe two approaches for analysis of this probability. Both approaches fundamentally consider segment fragility and correlations, but in different ways.

3.1 Monte Carlo Simulation-Based Approach

The approach begins with the definition of limit state function, *Z*:

$$Z = C - D \tag{2}$$

where *C* is capacity and *D* is demand. Note that *C* and *D* are spatially correlated random variables assumed to be log-normally distributed, hence *Z* is also log-normal. Moments of the log normal distributions are constant within a reach, but there are between-segment variations in capacity and demand, which are driven by the respective correlation functions. The system failure probability is evaluated as follows:

1. Populate two sets of uncorrelated normal random variables, which will be used later for capacities and demands, with a sufficient number of realizations (here: 50,000) for each segment.
2. Construct symmetric matrices of correlation coefficients for demand ($\mathbf{K}_D$) and capacity ($\mathbf{K}_C$), as given in Kwak et al. [14].

$$\mathbf{K}_D = \begin{bmatrix} 1 & (\rho_D)_{12} & \cdots & (\rho_D)_{1n} \\ (\rho_D)_{21} & 1 & \cdots & (\rho_D)_{2n} \\ \vdots & \vdots & \ddots & \vdots \\ (\rho_D)_{n1} & (\rho_D)_{n2} & \cdots & 1 \end{bmatrix}$$
$$\mathbf{K}_C = \begin{bmatrix} 1 & (\rho_C)_{12} & \cdots & (\rho_C)_{1n} \\ (\rho_C)_{21} & 1 & \cdots & (\rho_C)_{2n} \\ \vdots & \vdots & \ddots & \vdots \\ (\rho_C)_{n1} & (\rho_C)_{n2} & \cdots & 1 \end{bmatrix} \tag{3}$$

where $(\rho_D)_{ij}$ and $(\rho_C)_{ij}$ are correlation coefficients between segments i and j for demand and capacity, respectively.

3. Use Cholesky decomposition (e.g., [18]) to modify the realizations generated in (1) to exhibit the desired spatial correlation structure developed in (2).
4. Transform the random variables from (3) to demands and capacities with appropriate units. This can be expressed in terms of a generic variable (Y) that both represents demands (e.g., ground shaking level for earthquakes, water elevation for high-water events) and the output of capacity functions.
5. Compute the limit state Z (Eq. 2) for each segment for each realization.
6. The damage state of the system is taken as 'failure' if any segment has capacity lower than demand ($Z < 0$) within the system.
7. Calculate the fraction of realizations for which $Z < 0$, which is an estimate of the system probability of failure.

Figure 2 illustrates the procedure for evaluating the system failure probability using the Monte Carlo simulation-based approach.

3.2 Level-Crossing Statistics Method

The Monte Carlo simulations presented in the previous section are computationally demanding for large systems. A conceptually similar alternative that is less computationally demanding is described here. It involves computing the statistics of the limit state function (i.e., the distribution function and spatial correlation function) for segments within a reach using the FORM [19] and then computing the reach failure probability using level-crossing statistics. Reach failure probabilities can then be extended to uni-modal bounds on system failure probabilities. The steps involved in this method are outlined below (see Vrouwenvelder, [11] or Jongejan and Maaskant, [13] for further details).

1. For each reach, define a representative segment having probability density functions (PDFs) for capacity and demand. Limit state function, Z, is the difference between capacity and demand (Eq. 2), and is generally taken as log-normal.
2. Given the demand and capacity PDFs from (1), calculate the conditional failure probability [P(F_{Seg}|E)], reliability index (β_{Seg}), and influence coefficients of the segment using FORM. Reliability index and failure probability are related as:

$$\mathrm{P}\left(F_{Seg}|E\right) = \mathrm{P}(Z < 0) = \Phi\left(-\beta_{Seg}\right) \quad (4)$$

where Φ is the standard normal cumulative distribution function. The influence coefficients [20] describe the relative weight of the demand (α_D) and capacity (α_C) distributions on the limit state function. This can be expressed by a linearized version of the limit state function at the design point (i.e., the point having the shortest distance from the limit state function to the origin in the standard normal space, [19]) as follows:

$$Z = \beta_{Seg} + \alpha_D \varepsilon_D + \alpha_C \varepsilon_C \quad (5)$$

where ε_C and ε_D are independent, standard normal variables. The squared sum of α_C and α_D is unity (i.e. $\alpha_D^2 + \alpha_C^2 = 1$).

3. Calculate the failure probability of the reach on the basis of level-crossing statistics. In this step an approximate version of the spatial correlation of the limit state function, $\rho_Z(x)$, is taken as the weighted sum of the correlation functions for capacity and demand ($\rho_C(x)$ and $\rho_D(x)$, respectively), as follows:

$$\rho_Z(x) = \alpha_C^2 \rho_C(x) + \alpha_D^2 \rho_D(x) \quad (6)$$

where x is separation distance between two points. The failure probability of a reach [P(F_R|E)] can now be approximated by:

$$\mathrm{P}(F_R|E) = 1 - \left(1 - \mathrm{P}\left(F_{Seg}|E\right)\right) \exp\left(-\frac{L}{2\pi}\sqrt{-\frac{d^2\rho_Z(0)}{dx^2}} \times exp\left(-\frac{\beta_{Seg}^2}{2}\right)\right) \quad (7)$$

where L is the reach length. Eq. (7) indicates a reach may be thought of, approximately, as a series system of independent, characteristics lengths, with a length (L_{Char}) given by:

$$L_{Char} = \mathrm{P}\left(F_{Seg}\right) \times \frac{2\pi}{\sqrt{-\frac{d^2\rho_Z(0)}{dx^2}}} \times \exp\left(\frac{\beta_{Seg}^2}{2}\right) \quad (8)$$

4. Calculate the conditional failure probability of the system combining reach conditional failure probabilities. Uni-modal bounds of system failure probability can be computed from reach failure probabilities using Eq. (1). When characteristic lengths are appreciably

shorter than reach lengths, we consider it acceptable to assume zero correlation between reaches, as discussed further in Section 5.4.

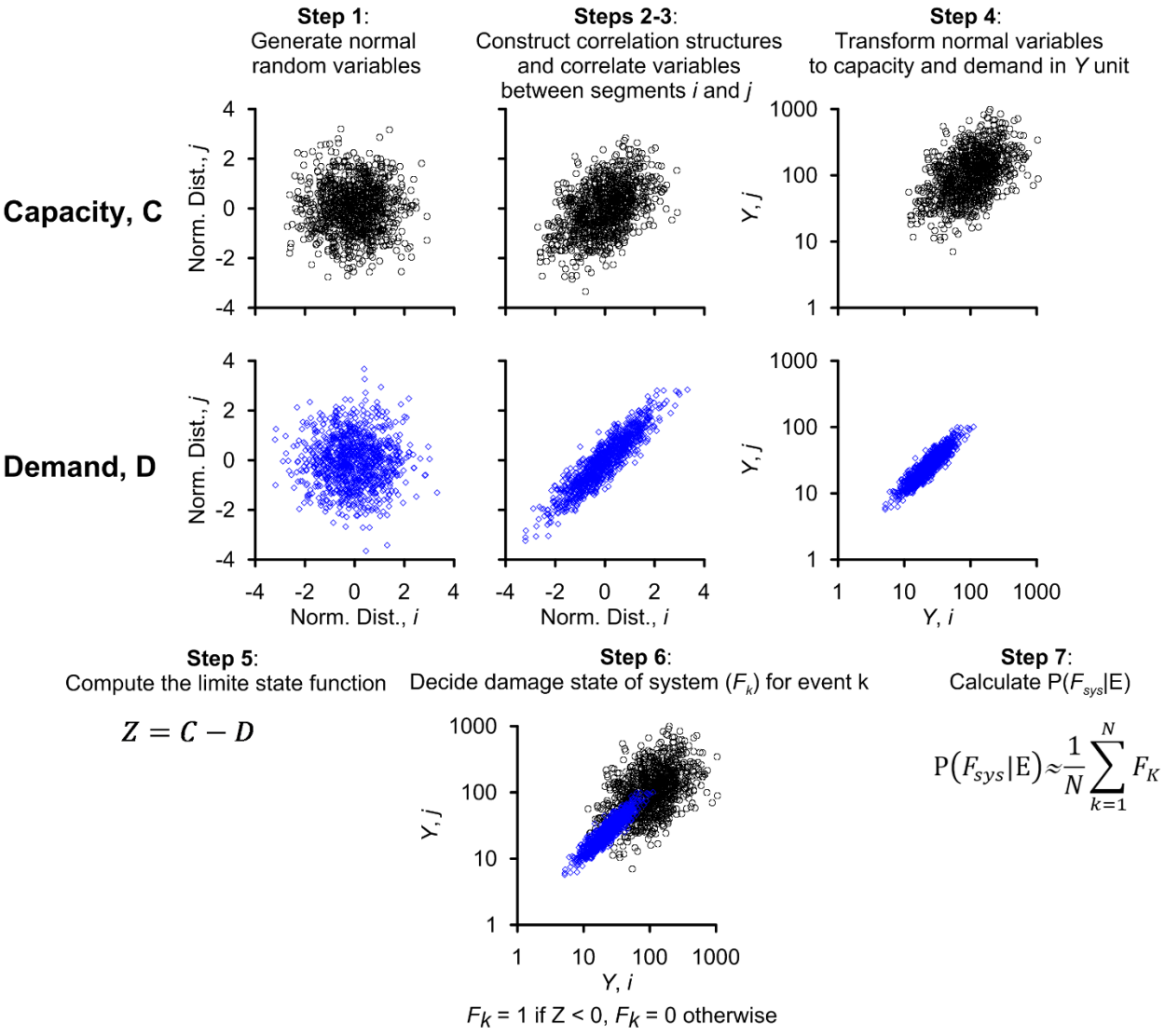

Figure 2. Illustration of procedure for system reliability analysis using Monte Carlo simulation. Adapted from Kwak et al. [15].

4. Input Models

4.1 Capacity Distributions

Fragility curves describe the probability of exceeding a specified damage limit state conditioned only on a ground motion intensity measure (in the case of earthquake demands) or other suitable demand parameters for high-water hazards. As illustrated in Figure 3, the capacity distribution for

a segment with deterministic demand can be taken as the derivative of its fragility curve [21], which has intensity measure Y on its abscissa. We take the seismic levee fragility (and hence capacity distribution) from the empirical models of Kwak et al. [8], which use the intensity measure of peak ground velocity, PGV in units of cm/s. These empirical models inherently consider failure modes contributing to observed levee deformations. For the considered data set, these primarily involve freeboard loss and/or levee cracking caused by slumping and shear deformations associated with liquefaction and cyclic softening of foundation soils, along with seismic slope instability and seismic compression. Figure 3 shows two example capacity distributions derived from these models. The distributions shown in Figure 3 are applicable for stiff soil (G_N=1 model; [8]) and for soft soil, high water, respectively.

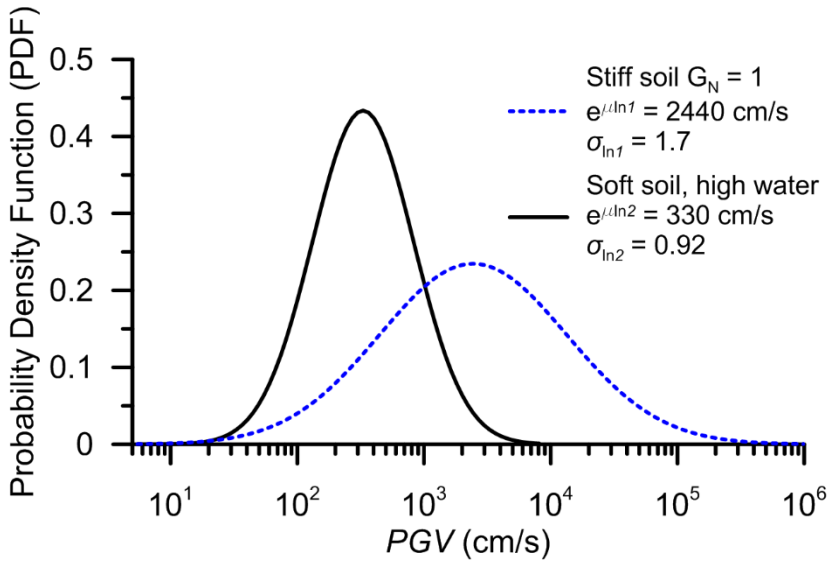

Figure 3. Example capacity distributions derived from empirical model of Kwak et al. [8]. μ_1 and μ_2 represent natural log mean capacities (the exponent is taken to convert to arithmetic units) and σ_{ln1} and σ_{ln2} represent standard deviations of capacity distributions.

For high-water conditions, possible failure mechanisms include underseepage (internal erosion), slope instability, and overtopping. In the application considered subsequently in this paper, we consider the internal erosion mechanism. We use the fragility relation shown in Figure 4 relating failure probability to vertical exit flow gradient, i [10]. Seepage analyses are used to relate water level (which comprises demand parameter Y in this case) to i, for the geometry and soil condition present in a particular levee reach. Hence, for the scenario high-water event (resulting from a storm in the river watershed) the demand parameter and the independent variable

used in the fragility curve are both represented by water level. Analyses of this sort are illustrated for an example problem in Section 5.

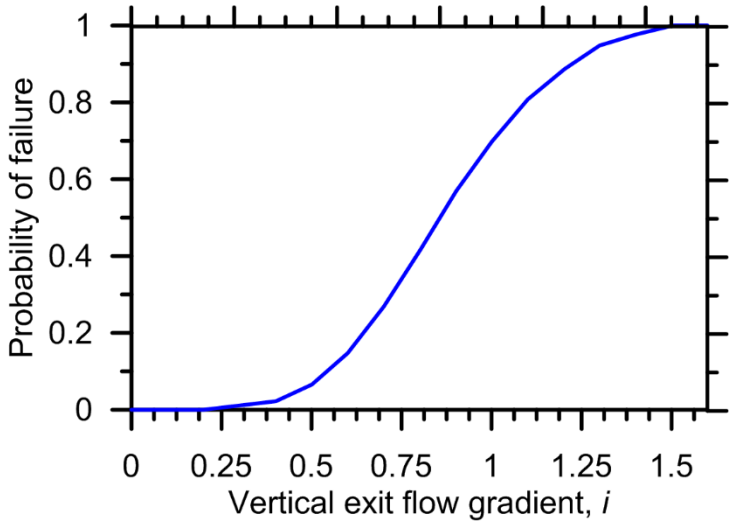

Figure 4. Fragility curve relating failure probability to vertical exit flow gradient, *i* (adapted from URS Corporation, Jack R. Benjamin & Associates Inc. [10]).

4.2 Correlation Models

Demand correlation for ground motion is taken from an empirical Markov-type correlation model by Jayaram and Baker [12]:

$$\rho_D(x) = \exp\left(\frac{-3x}{a_{DD}}\right) \tag{9}$$

where $a_{DD}$is a range parameter taken as 17.1 km for widely varying geologic conditions and 33 km for similar geologic conditions, and *x* is separation distance, as before. This form is referred to as a Markov correlation function. Figure 5 shows these two demand correlation models.

Demand correlation for high-water hazard is taken as unity, $\rho_D(x) = 1$. This is used because flood events are considered to raise the water level in a rather uniform manner in the water bodies bounded by levees. This assumption is considered reasonable when the levee system is bounding a common water body.

Capacity correlation, ρ_C, was estimated by Kwak et al. [14] using observations of the spatial correlations of damage states combined with correlations of seismic demand:

$$\rho_C(x) = \exp\left(\frac{-3x}{a_{CC}}\right) \tag{10}$$

where a_{CC} is the range parameter, which is 8.1 km for level ≥ 1 damage (effectively any perceptible damage level) and 3.2 km for level > 2 damage (severe damage). Lacking empirically derived capacity correlations for high water events in the literature, for reasons of simplicity, we apply the seismic correlation functions for levee capacities during high water events.

Markov correlation functions are not mean square differentiable (e.g., [22]), which is undesirable because it leads to unstable level-crossing statistics (the second derivative of the function at zero separation distance does not exist). This issue is less relevant in a Monte Carlo analysis because the separation distance between finite-length segments is larger than zero. Generally the resolution in the random field analysis (forward analysis) is consistent with the resolution that was used when deriving the correlation function from observations of damage.

The Gaussian correlation function provided in Eq. (11) is mean square differentiable, therefore finding a Gaussian correlation function that is "equivalent" to the Markov correlation function developed by Kwak et al. [14] is desirable. Ultimately, it would be desirable to re-derive demand and capacity correlation functions using the Gaussian function. In the meantime, an "equivalent" function is obtained by computing the probability of reach failure using the Markov function with the Monte Carlo method, then selecting a value of b_{CC} such that the same probability of reach failure is obtained using level-crossing statistics with the Gaussian function.

$$\rho_C(x) = \exp\left[-\left(\frac{3x}{b_{CC}}\right)^2\right] \tag{11}$$

As an example, consider Figure 6, which shows two limit state functions versus horizontal position along a 25 km linear levee system; one with a Markov correlation function and the other with a Gaussian function. The limit state function is selected to have a mean value of 0.5 and standard deviation of 0.2, and is assumed to be normally distributed. Failure is assumed to occur when the limit state function is lower than zero. The Markov type correlation function gives rise to high frequency variations in the limit state function, whereas the Gaussian limit state function is much smoother. The value of a_{CC} for the Markov function was set to 8.1 km following Kwak et al. [14], and the probability of failure was computed to be P_f = 0.23 using 1000 Monte Carlo

simulations, using the same resolution (i.e., segment length) used to derive the empirical correlation structure. The value of b_{CC} was then iteratively adjusted, and b_{CC} = 1.0 km was found to provide P_f = 0.23. These two correlation functions are therefore considered to be "equivalent". This approach is used to define appropriate equivalent Gaussian correlation structures for the capacity of each reach analyzed in Section 5.4. However, as long as mean-square differentiable, alternative functions may be used. The impact of this choice on the results of reliability analysis (i.e. the probability of failure, P_f) should be further investigated as additional data to constrain correlation functions become available.

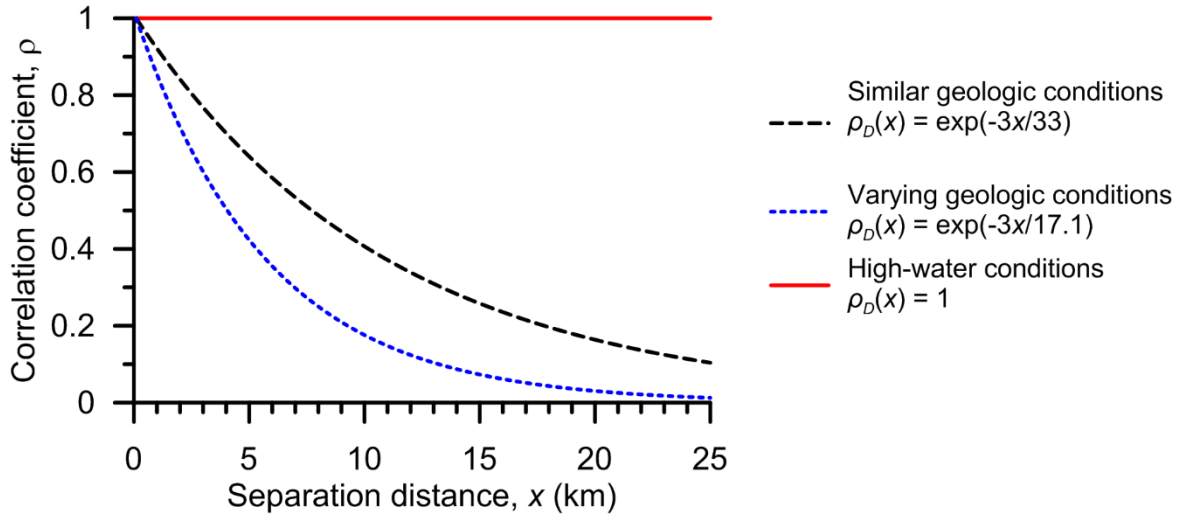

Figure 5. Demand correlation functions for both, seismic and high-water conditions.

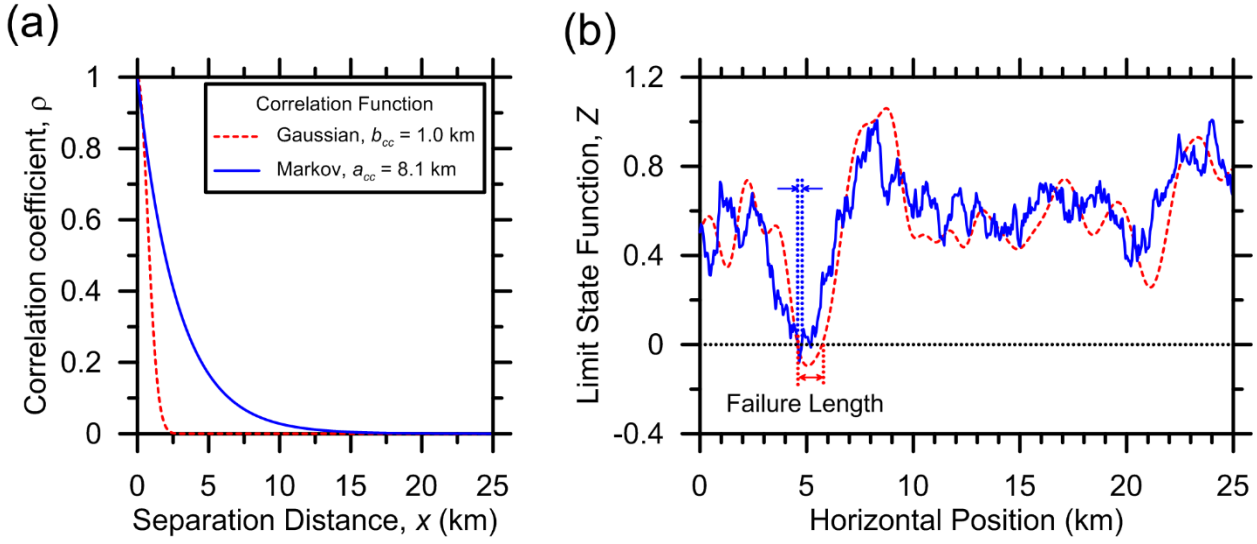

Figure 6. (a) Capacity correlation functions, and (b) their effect on lateral distribution of limit state function *Z*.

5. Example Application

5.1 Problem Description

We consider the levee system shown in Figure 7, which protects the town from flooding during high-water river flows. The river and levee are adjacent to the town through 'highland' (relatively firm soil conditions) and 'lowland' (soft soil) areas. The levee is 5 m in height and has a mean water level on the river side of 1 m above the levee base elevation – hence, the levee is assumed to be effectively continuously loaded. Due to the different foundation conditions, the highland and lowland levees have different side slopes of 1.5H:1V and 2H:1V, respectively, as shown in Figure 8. The time-averaged 30-m shear wave velocities in the two regions are 450 m/s and 200 m/s, respectively.

The study region is in an active seismic area, 15 km from a strike-slip fault having a scenario **M**6.5 earthquake. The area is also subject to water level rise in the river channel during storm events. Further details on the earthquake and high-water demands are provided next.

5.2 Scenario Demands

In this paper, we consider log-normally distributed scenario-based high-water level and seismic demands. Our failure probabilities are conditioned on those demand levels. We recognize that a more complete reliability analysis would convolve uncertain demands with levee fragilities to evaluate return periods on levee failure, but our work has not evolved yet to that point.

The scenario high-water event is assumed to result from a severe storm in the river watershed. The median water level rise (ΔD_W) for both reaches in the river near the subject town from this event is assumed to be 1.2 m (Figure 8a), with a natural log standard deviation of 0.2.

We take the scenario ground motion as the within-event PGV distribution along the levee alignment. There is some change with coordinate x due to varying site-source distance (taken as distance to surface projection of fault, R_{JB}) and site condition. Figure 9 shows the variation of 16^{th}, 50^{th}, and 84^{th} percentile demands (using the Boore et al. [23] ground motion model) with location along the levee. The origin of coordinate x is shown in Figure 7.

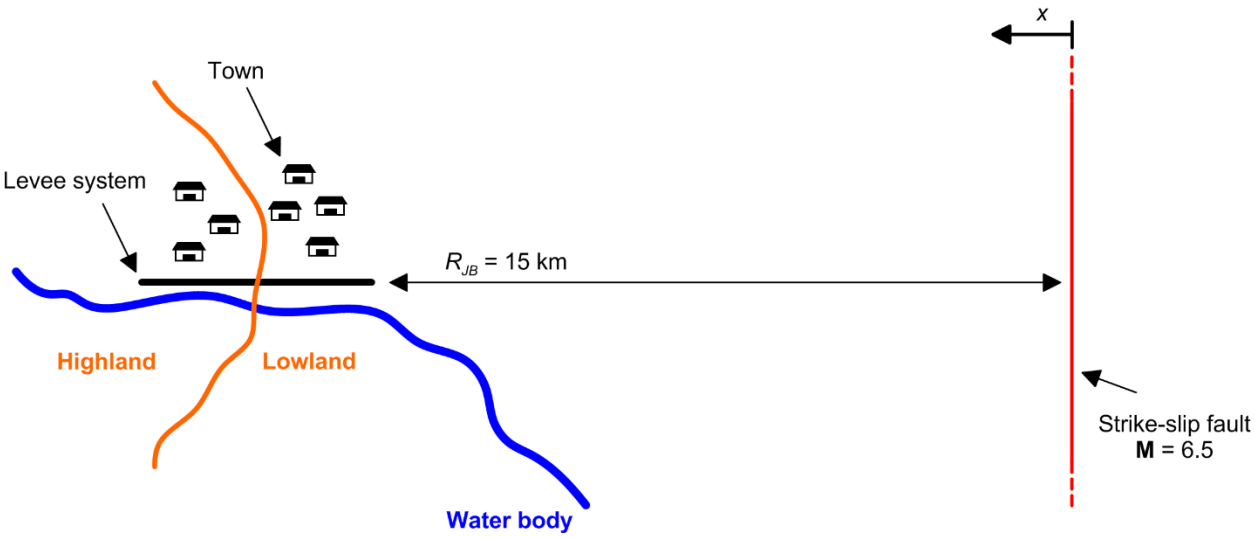

Figure 7. Schematic view of town protected by river-bounding levee passing over two geologic conditions and near an active fault.

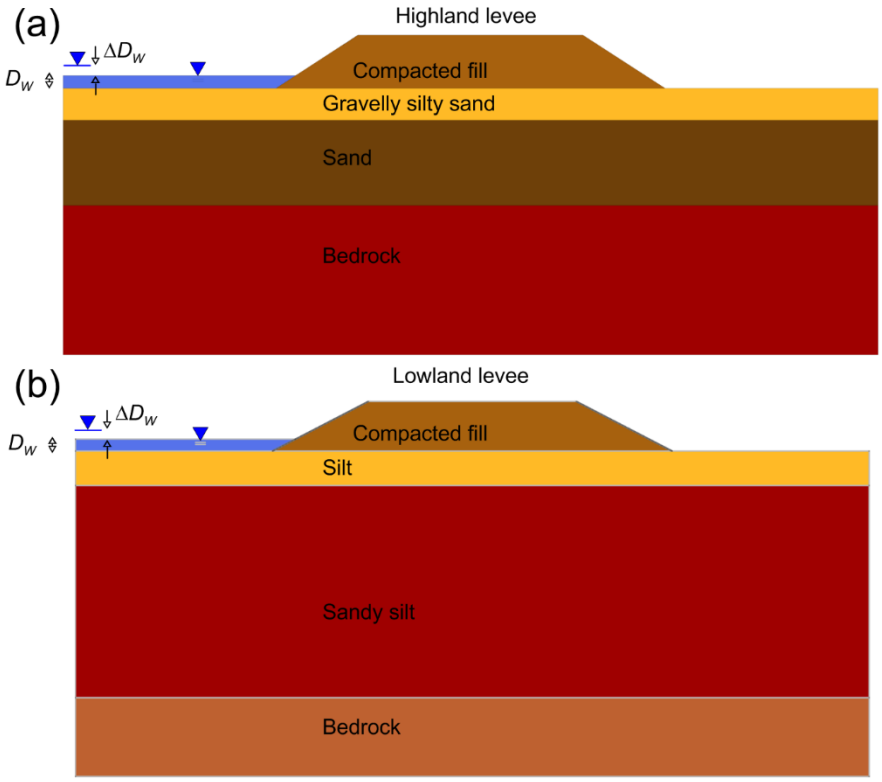

Figure 8. Cross sections of levees in: (a) highland area with mean water level plus mean water level rise, and (b) lowland area with mean water level.

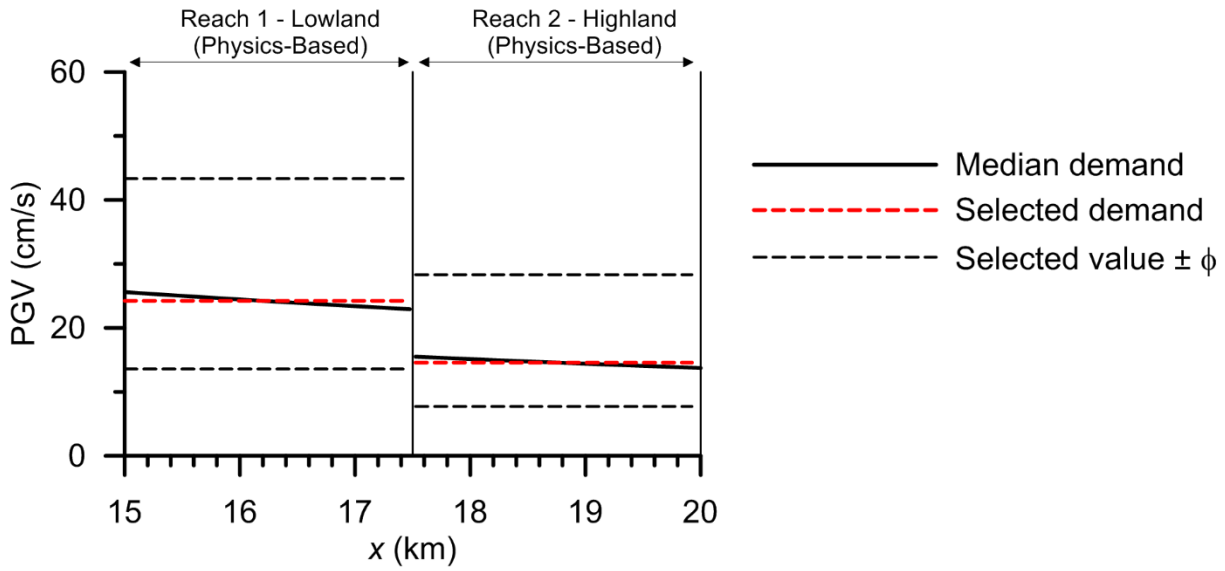

Figure 9. Variation of demand along the levee system. ϕ is within-event standard deviation [23].

5.3 Monte Carlo Approach

We apply the Monte Carlo approach (Section 3.1) using the following inputs:

- Seismic and high-water demand distributions are as described in Section 5.2.
- Seismic capacity distributions for highland and lowland areas are taken from the models of Kwak et al. [8] shown in Figure 3 as the G_N=1 model and the soft soil, high-water model, respectively.
- High-water capacity distributions are described below.
- Spatial correlation models for demand and capacity are as described in Section 4.2.

We develop fragility for high water level by combining the hydraulic gradient-based fragility (Figure 4) with reach-specific seepage analyses performed for both reaches (in lowland and highland areas). The steady-state seepage analyses were performed using the computer program Slide 7.0 [24] using the section geometry and hydraulic conductivities (K) shown in Figure 10. These seepage analysis results may be conservative for short-term flooding events, for which transient analyses would be more appropriate. Figure 10 also shows the resulting flow velocities for the mean high-water level of 2.2 m above levee base. Figure 11 shows the resulting internal erosion simulation-based data points along with fragility curves as a function of high water

elevation relative to levee base (D_W+ΔD_W). Both fragility curves are obtained fitting the data with a log-normal functional form, using the maximum likelihood estimation method [25].

Monte Carlo simulations (50,000 in total) applied to the seismic and high-water scenario events produce system failure probabilities of P(F_{sys}) = 0.098 and 0.11, respectively.

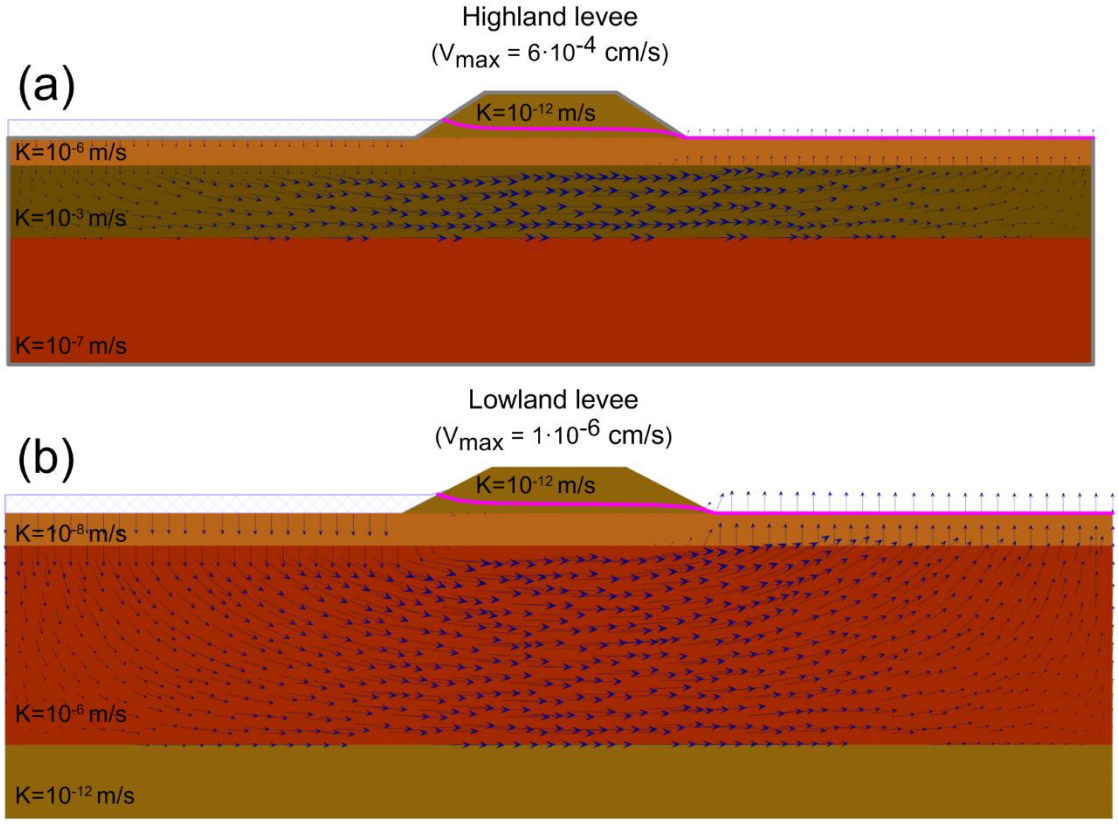

Figure 10. Computed fields of flow velocity beneath (a) highland and (b) lowland levees. Vector lengths are scaled relative to the maximum flow velocity (v_{max}).

5.4 Level-Crossing Statistics Approach and Characteristic Lengths

Recall that the level-crossing statistics approach is based on the assumption of constant limit state distributions within reaches (i.e. demands and capacities along the length of each reach are considered stationary). In the example problem, capacity distributions are constant within reaches, but demand distributions are variable with distance (x) as shown by the trend of median demand in Figure 9. Accordingly, we assign constant (spatially invariant) distributions to the two reaches as shown in Figure 9.

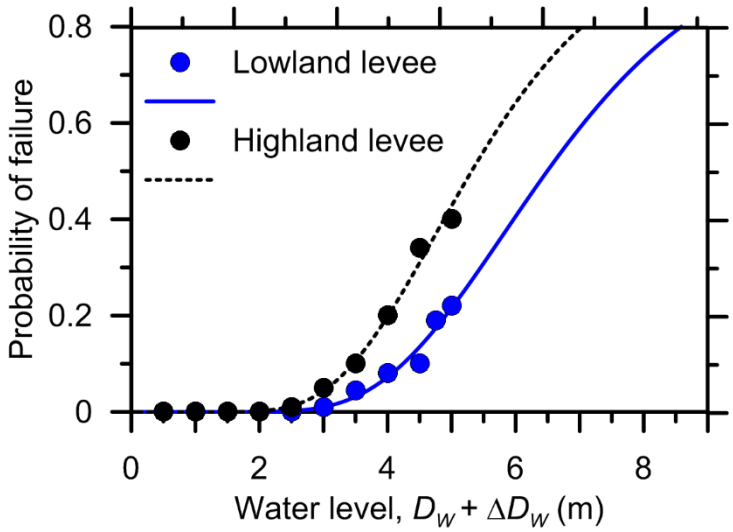

Figure 11. Internal erosion fragilities as a function of high water elevation relative to levee base. Dots represent data points obtained from seepage analyses, solid lines represent fitting curves obtained with a log-normal functional form, using the maximum likelihood estimation method.

Based on the demand and capacity distributions, results of the FORM analyses within the two reaches are given in Table 1. The higher failure probability for the highland, high water case results from the shorter flow path and faster flow velocities (Figure 10). Application of level-crossing statistics to the segment-level FORM results produces the reach conditional failure probabilities and characteristic lengths in Table 2.

Table 1. FORM analysis results for segment-level performance in conditioned scenario events E

Reach & Demand	$P(F_{seg}\|E)$	β_{seg}	α_D	α_C
Highland, seismic	0.002	2.81	0.36	-0.93
Highland, high water	0.011	2.28	0.52	-0.85
Lowland, seismic	0.008	2.40	0.53	-0.85
Lowland, high water	0.002	2.80	0.52	-0.85

Table 2. Results of level-crossing statistics for reach-level performance in scenario events.

Reach & Demand	$P(F_R\|E)$	L_{char} (km)
Highland, seismic	0.03	0.21
Highland, high water	0.09	0.33
Lowland, seismic	0.08	0.28
Lowland, high water	0.03	0.26

Having established the probability of failure for a single reach, we now turn our attention to computing the probability of failure of the multi-reach system. For simplicity, we assume that the limit state function for segments within one reach are uncorrelated with the limit state function for segments within an adjacent reach. Based on this assumption, the probability of system failure can be computed as:

$$P(F_{sys}|\mathrm{E}) = 1 - \prod_{i=1}^{N_R} \left[1 - P(F_{seg,i}|\mathrm{E})\right]^{L_i/L_{char}} \quad (12)$$

where N_R is the number of reaches. N_R is equal to two in the present application (Figure 9).

The assumption of statistical independence of the limit state function among reaches is justified when either of the following conditions is met:

1. The levee system exhibits an abrupt transition between reaches that occurs, for example, at the transition between two geologic units. This condition provides a physical justification for assuming that the limit state function is uncorrelated among reaches.
2. The characteristic lengths are significantly shorter than the reach length. In this case, any spatial correlation that exists at the contact between two reaches will not significantly influence the system failure probability.

For cases in which neither of these conditions are met, P(F_{sys}|E) will be lower than computed using Eq. (12), which therefore provides a conservative estimate. Eq. (12) constitutes one of two unimodal bounds given in Eq. (1). The other unimodal bound assumes that the limit state function is perfectly correlated among reaches. We believe the solution will generally lie closer to that provided by Eq. (12) for geotechnical failure mechanisms because the limit state function is likely closer to being statistically independent than perfectly correlated among reaches for typical levee systems. This is especially so when demands exhibit spatial correlation over larger distances than capacities, which we consider to be a generally reasonable assumption.

Based on the use of Eq. (12), the conditional system failure probabilities for the two demand scenarios are:

- Seismic, P(F_{sys}|E) = 0.096
- High-water, P(F_{sys}|E) = 0.10

These failure probabilities compare favorably to results of Monte Carlo analysis (0.098 and 0.11 for seismic and high-water, respectively).

6. Conclusions

We describe two methods for reliability analysis of spatially distributed systems subjected to spatially variable and uncertain demands. The intended application is levee systems used for flood protection, and the reliability analyses are for high-water events (storm surge) and ground failure from earthquake shaking. The two methods are conceptually similar in that both utilize a limit state function defined as the difference between capacity and demand, which is described by its distribution and spatial correlation models.

One method randomly samples demands and capacities according to their respective distribution and correlation functions, computes limit states for levee segments, and computes failure probabilities on the basis of the number of realizations in which at least one segment fails divided by the total number of realizations (thousands). This method can consider spatially varying demands and capacities, but is computationally intensive.

The other method (referred to as the level-crossing statistics method) discretizes a system into multiple reaches, calculates the probability of failure for each reach, and combines reach probabilities of failure to evaluate system probability of failure. The reach failure probability is calculated by estimating the limit state function for a representative segment (using the First Order Reliability Method), and then extending that result to the reach level using level-crossing statistics. We postulate that reach failure probabilities can be combined to evaluate system probability of failure by assuming statistical independence between reaches, provided reach lengths exceed characteristic lengths. The FORM method is efficient and effective when the limit state function may reasonably be approximated as constant over fairly long reach lengths. However, the Monte Carlo method may be needed when demand and/or capacity varies significantly along the system length and the limit state function is non-stationary over short lengths.

Application of the two methods is illustrated using a two-reach levee system providing continuous flood protection to a town, and subject to high water and earthquake hazards. The high-water hazard is assumed to result from internal erosion from underseepage. The seismic hazard

pertains to freeboard loss and/or cracking caused by slumping and shear deformations driven by liquefaction and/or cyclic softening of levee and foundation soils.

Our example calculations show several attributes that reflect the characteristics of the input demand, capacity models, and correlation models:

1. The spatial correlation of the limit state function is much more strongly influenced by the capacity spatial distribution than the demand distribution. This reflects shorter correlation lengths for capacity.
2. Despite much stronger spatial demand correlations applied for the high-water scenario vs that for the seismic scenario, characteristic lengths for the two hazards are comparable. This outcome was caused in part by broadly similar influence coefficients of capacity and demand, together with the assumption of a common capacity correlation model for both failure modes, which may not be generally applicable. Field performance data has not yet been analyzed to develop capacity correlation models for high-water hazards.
3. For the example considered, results of the Monte Carlo and level-crossing statistics methods are generally comparable. It is unknown at this time how general this finding may be.

Two important aspects of the level crossing statistics method introduced in this paper are: (1) the conversion of Markov-type spatial correlation models for demand to Gaussian functions, and (2) considerations in the analysis of system reliability given failure probabilities for individual reaches.

Acknowledgements

This work was supported by California Department of Water and Resource (CA-DWR) under contract number 4600008849. This funding source is gratefully acknowledged. Any opinions, findings, and conclusions or recommendations expressed in this material are those of the authors and do not necessarily reflect those of the CA-DWR.

References

[1] Larson LW. The great USA flood of 1993. IAHS Conference - Destructive Water: Water-Caused Natural Disasters - Their Abatement and Control. Anaheim, California, USA;

1996.

[2] Sills GL, Vroman ND, Wahl RE, Schwanz NT. Overview of New Orleans levee failures: lessons learned and their impact on national levee design and assessment. J Geotech Geoenviron Eng 2008;134:556-65.

[3] Briaud JL, Chen HC, Govindasamy AV, Storesund R. Levee erosion by overtopping in New Orleans during the Katrina hurricane. J Geotech Geoenviron Eng 2008;134:618-32.

[4] Miller EA, Roycroft GA. Seismic performance and deformation of levees: four case studies, J Geotech Geoenviron Eng 2004;130:344–54.

[5] Sasaki Y. River dike failures during the 1993 Kushiro-oki earthquake and the 2003 Tokachioki Earthquake. Earthquake Geotechnical Case Histories for Performance-Based Design, T. Kokusho (editor); 131–57; 2009.

[6] Sasaki Y, Towhata I, Miyamoto K, Shirato M, Narita A, Sasaki T, Sako S. Reconnaissance report on damage in and around river levees caused by the 2011 off the Pacific coast of Tohoku earthquake. Soils and Foundations 2012;52:1016-32.

[7] Green RA, Allen J, Wotherspoon L, Cubrinovski M, Bradley B, Bradshaw A, Cox B, Algie T. Performance of Levees (Stopbanks) during the 4 September 2010 Mw 7.1 Darfield and 22 February 2011 Mw 6.2 Christchurch, New Zealand, Earthquakes. Seismol Res Lett 2011;82:939-49.

[8] Kwak DY, Stewart JP, Brandenberg SJ, Mikami A. Characterization of seismic levee fragility using field performance data. Earthq Spectra 2016a;32:193–215.

[9] Zimmaro P, Kwak DY, Stewart JP, Brandenberg SJ, Balakrishnan A, Jongejan R, Ausilio E, Dente G Xie J, Mikami A. Procedures from international guidelines for assessing seismic risk to flood control levees. Earthq Spectra 2017; DOI:10.1193/072316EQS117EP.

[10] URS Corporation, Jack R. Benjamin & Associates Inc. Levee vulnerability, Tech. Memo. Delta Risk Management Strategy. Final Phase 1, Oakland, California, USA; 2008.

[11] Vrouwenvelder T. Spatial effects in reliability analysis of flood protection systems. In Second IFED Forum. Lake Louise, Canada; 2006.

[12] Jayaram N, Baker JW. Correlation model for spatially distributed ground-motion intensities. Earthq Eng Struct Dyn 2009;38:1687–708.

[13] Jongejan RB, Maaskant B. Quantifying Flood Risks in the Netherlands. Risk Analysis 2015;35:252–64.

[14] Kwak DY, Stewart JP, Brandenberg SJ, Mikami A. Seismic levee system fragility considering spatial correlation of demands and component fragilities. Earthq Spectra 2016b;32:2207-28.

[15] Kwak DY, Jongejan R, Zimmaro P, Brandenberg SJ, Stewart JP. Methods for Probabilistic Seismic Levee System Reliability Analysis. ASCE-Geo-Risk 2017: Reliability-Based Design and Code Developments. Geotechnical Special Publication 283, 140-50; 2017; DOI: 10.1061/9780784480700.014.

[16] Zimmaro P, Stewart JP, Brandenberg SJ, Kwak DY, Jongejan R. System reliability of flood control levees. Proc. Third international conference on performance-based design in earthquake geotechnical engineering, July 16-19, Vancouver, Canada; 2017.

[17] Ang AH-S, Tang WH. Probability concepts in engineering: emphasis on applications in civil & environmental engineering. 2nd edition. Wiley, NY; 2007.

[18] Baecher GB, Christian JT. Reliability and statistics in geotechnical engineering. 1st edition. Wiley, NY; 2003.

[19] Rackwitz R. Reliability analysis—A review and some perspectives. Structural Safety 2001;23:365–95.

[20] Hasofer AM, Lind NC. Exact and Invariant Second-Moment Code Format. Journal of the Engineering Mechanics Division, ASCE 1974;100:111–121.

[21] Baker JW. Introducing correlation among fragility functions for multiple components, in Proc. 14th World Conf. Earthq. Eng., Beijing, China; 2008.

[22] Fenton GA, Griffiths DV. Risk assessment in geotechnical engineering, Wiley & Sons Inc; 2008.

[23] Boore DM, Stewart JP, Seyhan E, Atkinson GM. NGA-West 2 equations for predicting PGA,

PGV, and 5%-damped PSA for shallow crustal earthquakes. Earthq Spectra 2014;30:1057–85.

[24] Rocscience Inc. Slide v7.0 - 2D limit equilibrium slope stability analysis, Toronto; 2015.

[25] Baker JW. Efficient analytical fragility function fitting using dynamic structural analysis. Earthq Spectra 2015;31:579–99.